Supporting Information

Yu et al. 10.1073/pnas.1112352108

SI Materials and Methods

Structure Determination and Refinement. The structure of *Tth*Dus was determined by the SAD (single-wavelength anomalous dispersion) method with the program SHELX (1, 2). Two molecules of *Tth*Dus were contained in an asymmetric unit. To monitor the refinement, a random 7% subset of all reflections was set aside for calculation of R_{free} factor. After several cycles of refinement with the program phenix.refine (3) and manual fitting with the program COOT (4), the crystallographic R and R_{free} factors converged to 16.8% and 20.2%, respectively.

The crystal structure of *Tth*Dus in complex with *Tth*-tRNA^{Phe} was determined by the MRSAD method using the structure of *Tth*Dus as a search model and Se atoms as anomalous scatterers with the program PHASER (5). The model of the bound tRNA was built manually based on electron density. A random 8% subset of all reflections was set aside for calculation of R_{free} factor to monitor the refinement. Jelly body refinement was performed with REFMAC 5.6 (6) for protein, and then simulated annealing refinement was performed with CNS 1.3 (7) for the tRNA model using ribose puckering and Watson-Crick base pair restraints. The structure was refined at a resolution of 3.51 Å. After several cycles of refinement with the program phenix.refine and CNS 1.3, in which noncrystallographic symmetry restraints were applied to each complex in the asymmetric unit, and manual fitting with the program COOT, the R- and R_{free}- factors were converged to 30.0% and 32.0%, respectively (Table S1).

The crystal structure of the *Tth*Dus-tRNA fragment complex was determined at 1.95 Å resolution by the molecular replacement method using the structure of *Tth*Dus as a search model with the program MOLREP (8). To monitor the refinement, a random 4% subset of all reflections was set aside for calculation of the R_{free} factor. After several cycles of refinement with phenix.refine and manual fitting with COOT, the base and ribose moieties of G18, G19, the target uridine at position 20, and A21 were defined based on electron density. The model of *Tth*Dus-tRNA fragment complex was refined with the program REFMAC. Finally, R- and R_{free}- factors were converged to 18.1% and 21.9%, respectively (Table S1).

Preparation of tRNA for Evaluation of Dihydrouridine Formation. The *yjbN* gene, including its promoter region, was amplified from *E. coli* (MG1655) genomic DNA using the forward primer 5′-NNGAATTCGACAGGCGCTTCCTGTTGTTATG-3′ and reverse primer 5′-NNNGGATCCTTAACGCTTATCCGCCACCAGTTTG-3′. The PCR product was inserted into *Bam*HI and *Eco*RI sites of the pMW118 vector (Nippon Gene), which was used for complementing the deleted *yjbN* gene.

The *E.coli yjbN* knockout strain (*E. coli* Δ*yjbN*), harboring the desired vector to complement the *yjbN* gene, was grown at 37 °C for 18 h in LB medium supplemented with 100 mg L^{-1} ampicillin and 50 mg L^{-1} kanamycin. The cells were collected by centrifugation at 4,500 × *g* for 20 min, and then the total tRNA was extracted by acidic-phenol method. The cells were resuspended in a buffer containing 50 mM sodium acetate (pH 5.2) and 10 mM magnesium acetate, followed by phenol treatment overnight. The aqueous layer was collected and mixed with chloroform (1/5 of the volume of the aqueous layer). The aqueous layer was collected again, and total RNA was precipitated by isopropanol precipitation using 0.3 M sodium acetate (pH 5.2) and 50% isopropanol. The precipitate was resuspended, followed again by phenol treatment and chloroform treatment. The aqueous layer was collected, and then subjected to isopropanol precipitation with 0.3 M sodium acetate (pH 5.2) and 33% isopropanol. The resultant solution was collected, and isopropanol was added to a final concentration of 50%. The precipitate after centrifugation at 8,000 × *g* was collected as a total tRNA. The extracted tRNA was digested with RNase T1, and then analyzed by capillary liquid chromatography nano-electrospray ionization/mass spectrometry, which included a linear ion trap-orbitrap hybrid mass spectrometer (LTQ Orbitrap XL; Thermo Fisher Scientific), a custom-made nanospray ion source, and a splitless nano-high-performance liquid chromatography system (DiNa; KYA Technologies).

Mass Spectrometric Analysis of RNA in *Tth*Dus-tRNA Complex Formed in *E. coli* Cells. The purified *Tth*Dus-tRNA complex formed in *E. coli* cells was treated with acid-phenol/chloroform (5:1, pH 4.5; Ambion, Foster City, CA). The aqueous layer was collected by centrifugation, and the RNA was collected by ethanol precipitation with 0.3 M sodium acetate (pH 5.2) and 70% ethanol at −30 °C, followed by washing with 70% ethanol and drying. The purified RNA was subjected to Urea-PAGE. The RNA molecules contained in the major bands were extracted from the gel using the Electro-Separation System (Whatman), followed by ethanol precipitation. The obtained RNA was analyzed by capillary liquid chromatography nano-electrospray ionization/mass spectrometry as described above.

Expression and Purification of YjbN and Its K138A Mutant. The genes of YjbN and K138A mutant were amplified using KOD-Plus DNA polymerase (Toyobo), with the vector for the complementation experiment (see above) as the template and the synthesized primers (YjbN-S: 5′-NNNNNCCATGGCCCCTGAAAAAACTGACGTTCACTGGAGTG-3′, and YjbN-AS: 5′-NNNNCTCGAGACGCTTATCCGCCACCAGTTTGAGC-3′). The PCR products were inserted into the *Nco*I and *Xho*I sites of the pET28b vector (Merck), in which the His_6 tag was attached at the C terminus.

YjbN and K138A mutant were expressed in *E. coli* strain B834 (DE3) in LB medium supplemented with 100 μg mL^{-1} kanamycin. Expression was induced by addition of 0.5 mM IPTG at the early stationary phase of culture and processed for 18 h at 25 °C. The collected cells were resuspended in buffer [50 mM Hepes-NaOH (pH 7.5), 500 mM KCl, 1 mM $MgCl_2$, 10% glycerol, 7 mM β-mercaptoethanol], and disrupted with a sonicator (Branson). The supernatant was loaded onto a HisTrap HP column (GE Healthcare), and then the adsorbed protein was eluted with a linear gradient of 0 mM–500 mM imidazole. Fractions containing the desired protein were collected and dialyzed against the resuspension buffer. The concentrations of YjbN and the K138A mutant were determined by the absorption at a wavelength of 280 nm.

Isothermal Titration Calorimetry (ITC). All ITC measurements were carried out with a Nano ITC Low Volume isothermal titration calorimeter (TA Instruments). The cell was filled with YjbN K138A mutant with a concentration of 228 μM, and a syringe was filled with 1.87 mM FMN. FMN was injected 25 times in aliquots of 2 μL over 300 s. The data obtained were analyzed with the program Nano Analyzer (TA Instruments).

1. Sheldrick GM (2008) A short history of SHELX. *Acta Crystallogr A* 64:112–122.
2. Sheldrick GM (2010) Experimental phasing with SHELXC/D/E: combining chain tracing with density modification. *Acta Crystallogr D* 66:479–485.
3. Adams PD, et al. (2010) PHENIX: a comprehensive Python-based system for macromolecular structure solution.*Acta Cryst* D66:213–221.
4. Emsley P, Cowtan K (2004) COOT: model-building tools for molecular graphics. *Acta Crystallogr D* 60:2126–2132.
5. McCoy AJ, et al. (2007) Phaser crystallographic software. *J Appl Crystallogr* 40:658–674.
6. Murshudov GN, Vagin AA, Dodson EJ (1997) Refinement of macromolecular structures by the maximum-likelihood method. *Acta Crystallogr D* 53:240–255.
7. Brunger AT, et al. (1998) Crystallography & NMR system: a new software suite for macromolecular structure determination. *Acta Crystallogr D* 54:905–921.
8. Vagin A, Teplyako A (1997) MOLREP: an automated program for molecular replacement. *J Appl Cryst* 30:1022–1025.

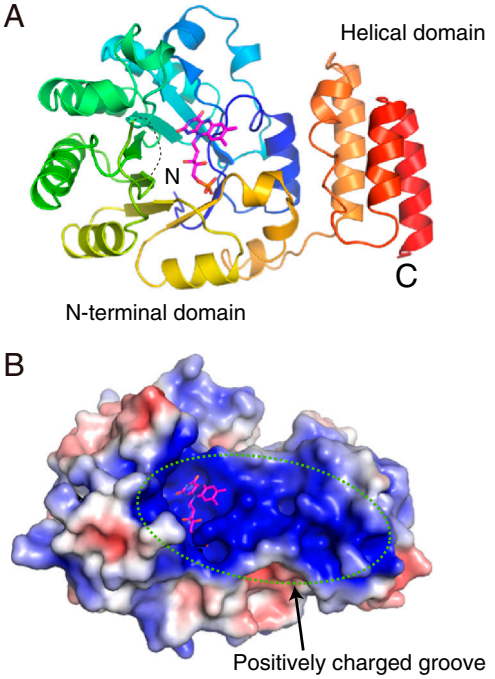

Fig. S1. Overall structure of *Tth*Dus. (*A*) Ribbon diagram of *Tth*Dus. The ribbon model is colored according to the sequence from blue at the N terminus to red at the C terminus. FMN is shown as sticks. The dotted line indicates the disordered region of Ala171-Ile180. (*B*) Electrostatic surface potential of *Tth*Dus. The orientation is identical to that of Fig. 1*A*. Positively and negatively charged surfaces are colored blue and red, respectively ($\pm 5\ k_b T e_c^{-1}$). The green circle indicates the positively charged groove.

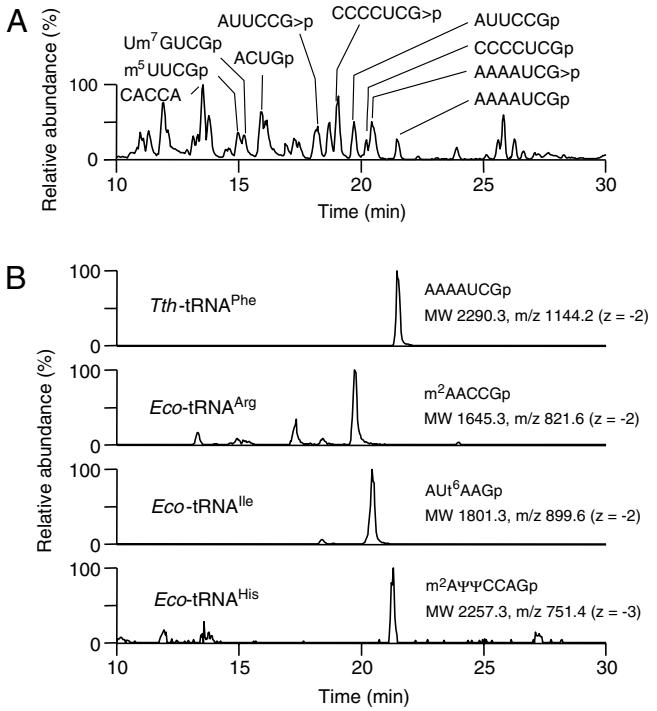

Fig. S2. Mass spectrometric analysis of the RNA contained in the purified *Tth*Dus-tRNA complex. (*A*) The base peak chromatogram of the RNA fragment obtained by RNase T1 digestion. The sequences of the fragments identified as derived from *Tth*-tRNA^{Phe} are indicated. "*>p*" denotes a cyclic phosphate. (*B*) Identified fragments derived from tRNA from *E. coli*. The AAAAUCGp fragment from *Tth*-tRNA^{Phe} is also shown.

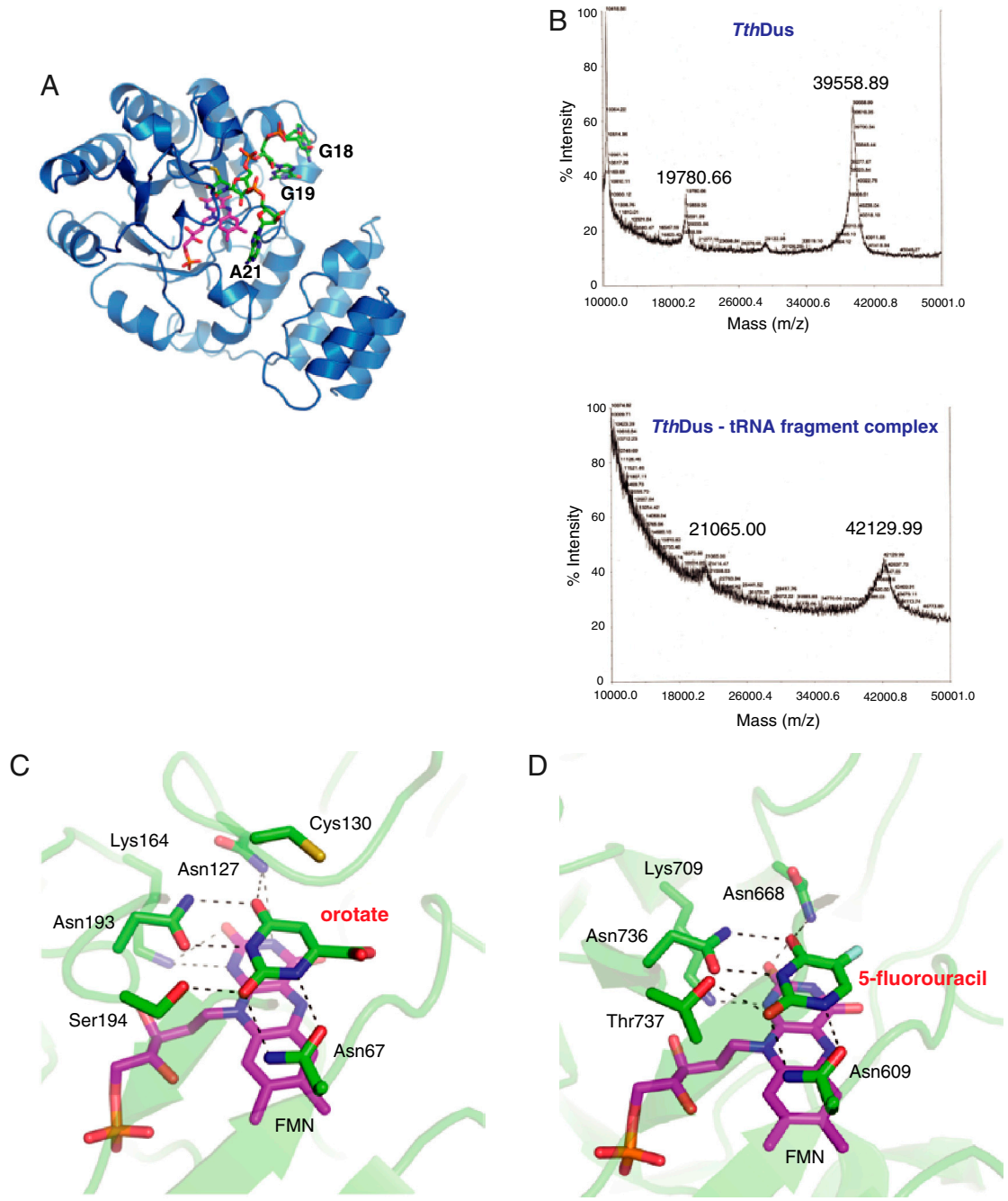

Fig. S3. Supporting information for the crystal structure of *Tth*Dus-tRNA fragment complex (*A*) Overall structure of *Tth*Dus-tRNA fragment complex. tRNA fragment and FMN are shown as green and pink sticks, respectively. Cys93 is also shown as sticks. (*B*) Results of time-of-flight mass spectrometry (TOF-MS) of the purified *Tth*Dus (top) and *Tth*Dus-tRNA fragment complex (bottom). (*C*) Substrate recognition of dihydroorotate dehydrogenase (DHOD, PDB 2DOR) (*D*) Substrate recognition of dihydropyrimidine dehydrogenase (DHPDH, PDB 1H7X).

A

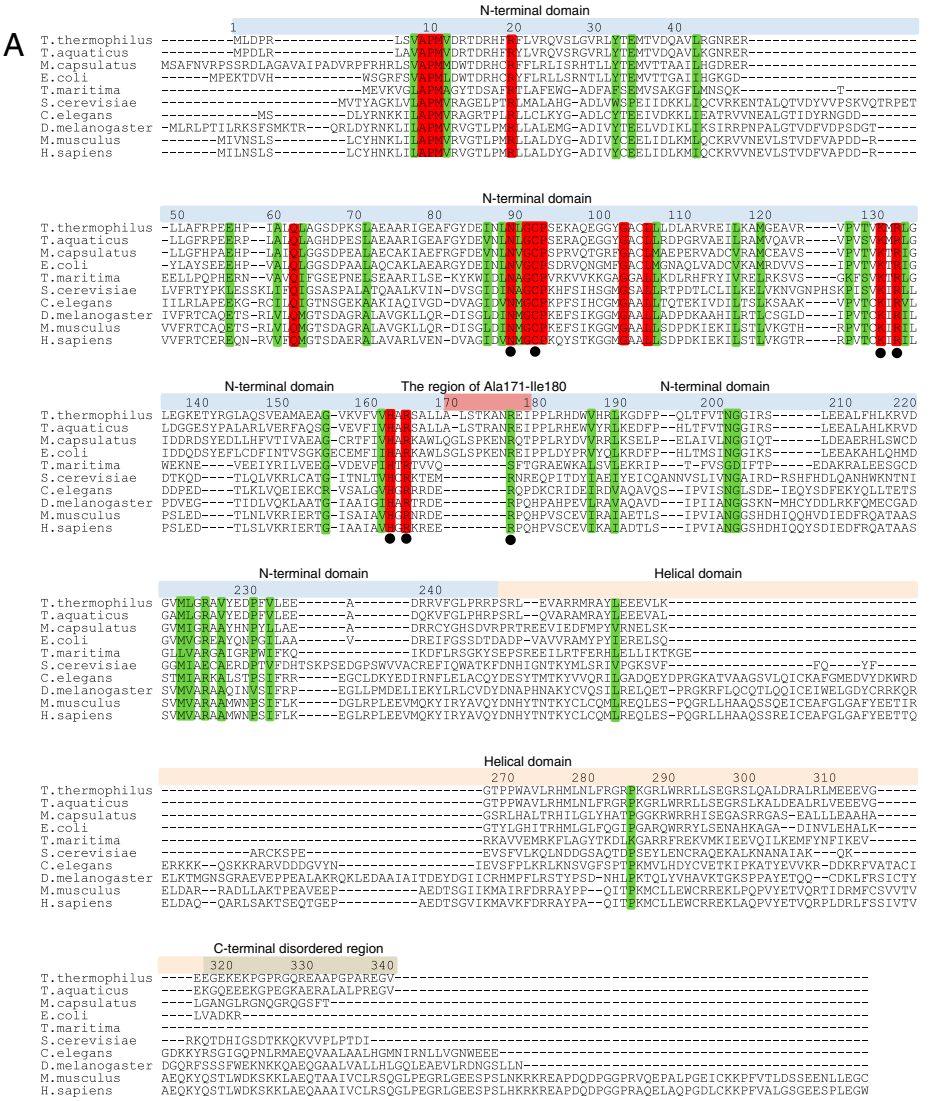

B

*Tth*Dus	*Ec*YjbN
N90A	N96A
C93A	C99A
C93S	C99S
K132A	K138A
R134A	R140A
H164A	H171A
R166A	R173A
R178A	R186A

Fig. S4. Sequence alignment of *Tth*Dus and Dus family proteins (*A*). Completely conserved residues and conservatively mutated residues are shown in red and green, respectively. *T. thermophiles*, *Thermus thermophilus*; *T. aquaticus*, *Thermus aquaticus*; *M. capsulatus*, *Methylococcus capsulatus*; *E. coli*, *Escherichia coli*; *T. maritima*, *Thermotoga maritima*; *S. cerevisiae*, *Saccharomyces cerevisiae*; *C. elegans*, *Caenorhabditis elegans*; *D. melanogaster*, *Drosophila melanogaster*; *M. musculus*, *Mus musculus*; *H. sapiens*, *Homo sapiens*. Circles represent substituted residues in the mutation analysis of *Ec*YjbN. (*B*) Correspondence between mutants of *Tth*Dus and *Ec*YjbN.

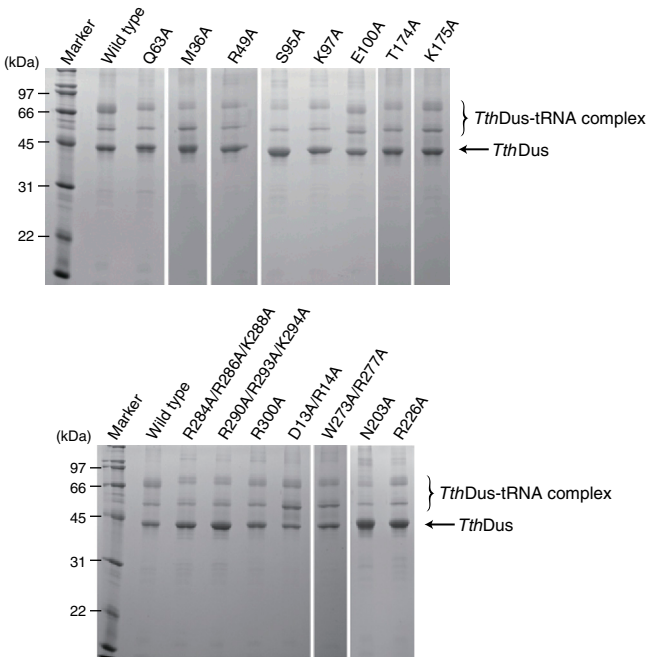

Fig. S5. SDS-PAGE of purified *Tth*Dus mutants, which were not shown in Fig. 4*A*.

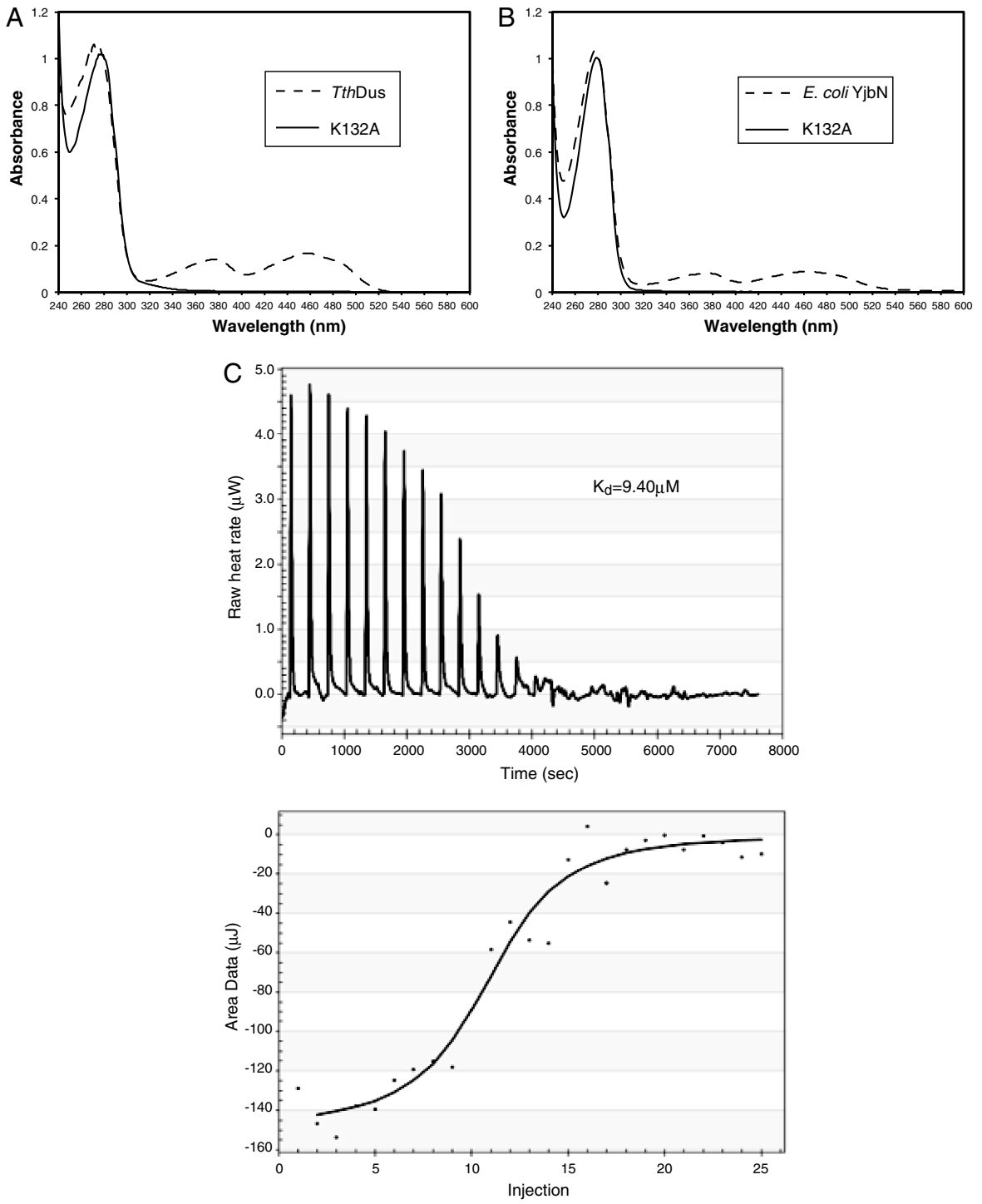

Fig. S6. Characterization of K132A mutants. (*A*) The absorption spectra of *Tth*Dus and its K132A mutant. (*B*) The absorption spectra of *Ec*YjbN and its K132A mutant. (*C*) Thermogram of the interaction between *Ec*YjbN K132A and FMN. The dissociation constant between *Ec*YjbN K132A and FMN was calculated to be 9.40 μM.

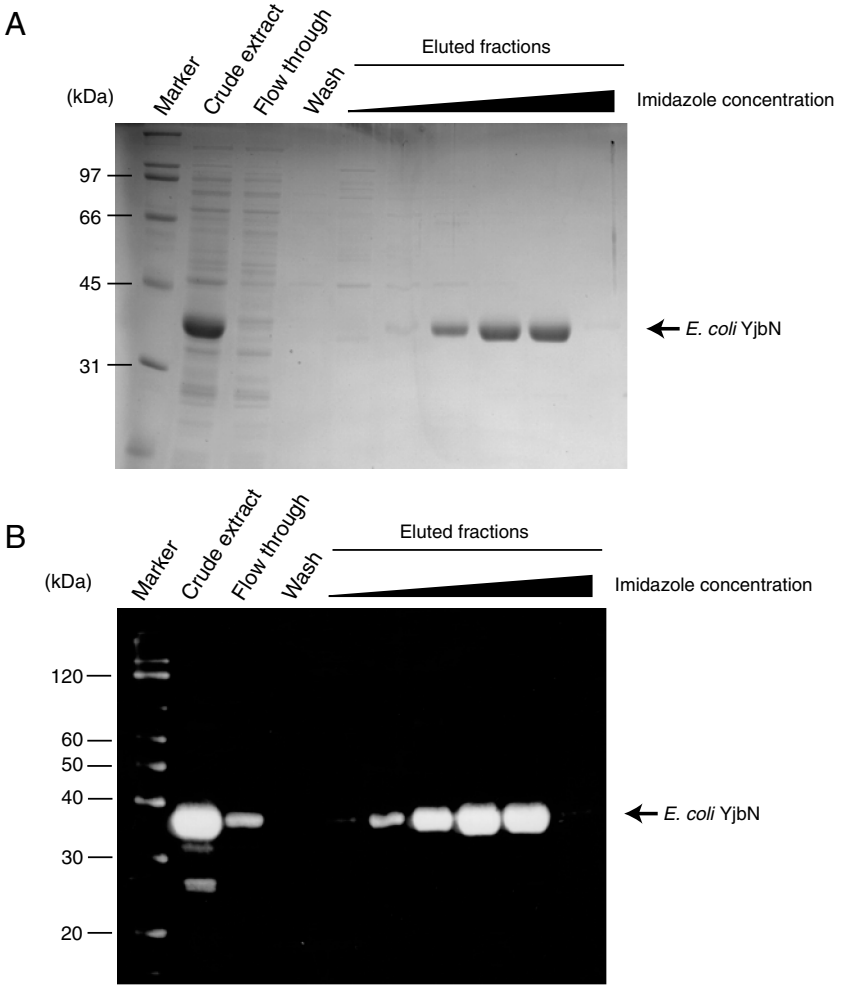

Fig. S7. SDS-PAGE (*A*) and Western blotting (*B*) of *E. coli* YjbN. Fractions obtained by Ni affinity chromatography were analyzed.

Table S1. Statistics for data collection and refinement

	SeMet *Tth*Dus	Native *Tth*Dus	*Tth*Dus-tRNA fragment	SeMet *Tth*Dus-tRNA
PDB code		3B0P	3B0U	3B0V
Data collection				
Beamline	Spring-8 BL41XU	PF NE3A	PF BL5A	PF BL5A
Wave length (Å)	0.9792	1.0000	1.0000	0.9788
Space group	*P*1	*P*1	*R*3	$P4_12_12$
Cell dimensions	$a = 43.6$ Å, $b = 60.3$ Å, $c = 67.3$ Å, $\alpha = 75.7°$, $\beta = 87.7°$, $\gamma = 70.5°$	$a = 42.0$ Å, $b = 60.2$ Å, $c = 67.0$ Å, $\alpha = 76.2°$, $\beta = 88.7°$, $\gamma = 70.7°$	$a = b = 126.6$ Å, $c = 112.7$ Å, $\alpha = \beta = 90°$, $\gamma = 120°$	$a = b = 118.9$ Å, $c = 319.6$ Å
Resolution * (Å)	50.00–2.30 (2.38–2.30)	19.77–1.70 (1.79–1.70)	19.80–1.95 (2.05–1.95)	48.60–3.51 (3.70–3.51)
R_{sym} * (%)	9.8 (40.3)	4.6 (45.7)	6.5 (52.8)	11.6 (53.1)
$\langle I/\sigma(I)\rangle$ *	16.4 (2.3)	17.9 (2.8)	18.4 (3.5)	17.1 (4.6)
Completeness * (%)	97.3 (94.0)	95.6 (91.7)	99.7 (98.6)	99.5 (97.1)
Multiplicity *	7.6 (6.5)	3.9 (3.7)	5.7 (5.6)	13.2 (11.8)
No. of observed reflections *	203,476	247,001 (32,524)	281,568 (40,009)	387,969 (47,935)
No. of unique reflections *	26,878 (2,590)	63,586 (8,907)	49,091 (7,132)	29,454 (4,077)
Refinement				
R-factor / *R*-free (%)		16.8/20.2	18.1/21.9	30.0/32.0
No. of protein atoms		4,901	4,992	5,020
No. of RNA atoms			170	3,122
No. of ligand atoms		62	62	62
No of water molecules		387	421	
rmsd				
Bond lengths (Å)		0.008	0.003	0.004
Bond angles (°)		1.08	0.707	0.9
Ramachandran-plot †				
Favored (%)		97.2	96.5	96.0
Allowed (%)		2.8	3.5	3.7
Disallowed (%)		0.0	0.0	0.3

*Values in parentheses are for the highest-resolution shell.
†RAMPAGE (1) was used for Ramachandran-plot analysis.

1 Lovell SC, et al. (2003) Structure validation by Calpha geometry: phi,psi and Cbeta deviation. *Proteins* 50:437–450.